https://doi.org/10.18321/ectj957

Effect of Different Pore-Forming Additives on the Formation of PVDF Microporous Membranes for Bucky-Gel Actuator

O.S. Morozov[1]*, S.S. Shachneva[2], B.A. Bulgakov[1,3], A.V. Babkin[1,3], A.V. Kepman[1,3]

[1]Department of Chemistry, Lomonosov Moscow State University, 1-3 Leninskie Gory, Moscow 119991, Russia
[2]Faculty of Materials Science, Lomonosov Moscow State University, 1-73 Leninskie Gory, Moscow 119991, Russia
[3]Institute of New Carbon Materials and Technologies (INCMaT), 1-11 Leninskie Gory, Moscow 119991, Russia

Article info

Received:
2 August 2019

Received in revised form:
26 October 2019

Accepted:
24 February 2020

Abstract

The microporous polyvinylidene fluoride (PVDF) membranes were prepared by the solvent evaporation method using 50 wt.% of different pore-forming additives: poly(1-ethyl-3-vinylimidazolium tetrafluoroborate) (PIL-BF_4), polyethylene glycol 3000 (PEG-3K) and 40000 (PEG-40K), dibutyl phthalate (DBP). The influence of used additive on morphology, porosity, degree of crystallinity, tensile properties, electrolyte uptake and ionic conductivity of the membranes were investigated. The maximum electrolyte uptake of 1-ethyl-3-methylimidazolium tetrafluoroborate ($EMImBF_4$) was 184 wt.% for the membrane prepared with PEG-40K, however, the membrane was fragile and unsuitable for practical use. The remaining membranes showed approximately the same porosity (45–48%) and electrolyte uptakes (169–175%). At the same time, the membranes significantly differed in mechanical properties and ionic conductivity. The membrane prepared with PIL-BF_4, unlike others, has a sponge-like structure and demonstrated high mechanical properties, namely tensile strength is 17.7 MPa and fracture strain is 132.5%. Bucky gel actuators were fabricated using membranes prepared with different additives. The blocking force of the actuators based on membranes with different additives decreased in the sequence of PIL-BF_4, DBP and PEG. The actuator based on the membrane prepared with PIL-BF_4 demonstrates a blocking force of 5.7 mN and a deformation of 1.35 % at 3 V DC.

1. Introduction

Polyvinylidene fluoride (PVDF) and its co-monomers are of the most studied and common polymers for membrane manufacturing. The special properties of PVDF include high radiation, chemical and thermal stability, and superior mechanical performance [1–5]. Applications of PVDF membrane technologies in diverse purification processes [6] such as water treatment [7, 8], gas separation [9], and environmental protection [10] are known. PVDF membranes have been implemented as an ion separators in electronic devices, including supercapacitors [11], sensors [12], actuators [13, 14], and lithium-ion batteries [6, 15–17]. PVDF membranes for the most common applications can be produced by non-solvent induced phase separation (NIPS) process and thermally induced phase separation (TIPS) [18]. Different PVDF membrane morphologies can be obtained by phase inversion of a polymer solution in a liquid bath with aliphatic alcohols or with water containing inorganic salt additives as a nonsolvent [15, 16]. In dry-cast preparation technique, process conditions such as temperature, drying rate, polymer concentration and chemical nature of nonsolvent define the final morphology of the membranes. Membrane microporous structure can be achieved by using polymeric pore-forming additive instead of nonsolvent. High-boiling common plasticizers such as dibutyl phthalate (DPB) [19] and tributyl citrate [20] or polymers such as polyethylene glycol (PEG) [21] and polyvinylpyrrolidone [22], and

*Corresponding author. E-mail: osmorozov@yandex.ru

others [23, 24] were utilized as pore formers. After the casting process, the additives are extracted by organic solvents from the membrane to form a porous structure. For electrochemical applications, a polymer gel electrolyte (PGE) is prepared by dry PVDF membrane saturation in the electrolyte. The pore size and its distribution, a fraction of open porosity, the interconnectivity of the pore domain, and the nature of the polymer matrix determine the uptake of electrolyte and the ion conductivity of the electrolyte membrane. PGEs have been developed to replace liquid electrolytes. Though they possess suitable mechanical properties and eliminate leakage problem, yet relatively low ionic conductivity limits their usage. The high ionic conductivity, thermal and chemical stability, a wide electrochemical window are the unique properties of ionic liquids (ILs), making them a good alternative to aqueous or solid electrolytes to prepare PGEs. Polymer gel electrolytes based on IL demonstrate room temperature conductivity above 10^{-3} S/cm, which is enough for practical use [25]. The simplest way to produce PVDF membrane for electroactive polymer actuators is the conventional dry-casting process [26]. However, the manufacturing of membranes from a mixture of polymer and IL, large ionic clusters are formed, and part of the IL may be in closed pores [27]. Therefore, it is more convenient to control the structure and properties of the membrane by introducing an additive during its manufacture. Previously we demonstrated the effectiveness of using poly(1-ethyl-3-vinylimidazolium tetrafluoroborate) (PIL-BF_4) as a pore-forming additive for the manufacture of a durable and highly porous PVDF membrane [28]. This study is focused on the comparison of different additives as a pore-former on the structure, mechanical and electrochemical properties of PVDF membranes, and the influence of the membrane properties on bucky-gel actuators performance.

2. Materials and Methods

2.1. General information

NMR spectra were recorded on a Bruker Avance III Ultrashield spectrometer at 600 MHz (^{1}H) and 151 MHz (^{13}C). All NMR samples were prepared in deuterated dimethylsulfoxide containing a trace amount of tetramethylsilane as a signal reference substance. Single wall carbon nanotubes (SWCNT) were purchased from the OCSiAl (Russia). PVDF was purchased from the Konstantinov Kirovo-Chepetsk Chemical Combine (Russia) as Fluoroplast-2. 1-Methylimidazole, 1-vinylimidazole, butyl bromide, ethyl bromide, sodium tetrafluoroborate and 2,2′-azobis(2-ethylpropionitrile) were purchased from commercial sources (Acros, Aldrich) and were used without further purification.

2.2. Membrane Preparation

In a round bottom 50 ml flask PVDF (1.0 g) and additive (1.0 g) were dissolved in 10 ml of *N,N*-dimethylformamide (DMF) at 100 °C. Dissolved air was removed from the casting solutions by ultrasonication for 30 min. Degassed solutions were cast on Petri dishes (Ø 9 cm) and put into preheated to 100 °C forced ventilation oven for 3 h. Then dry polymer films were removed from Petri dishes and weighted. The films were extracted by acetonitrile to remove pore-forming additives several time to achieve PVDF membranes.

2.3. Synthesis of 1-ethyl-3-vinylimidazolium tetrafluoroborate

To a 500 ml flask containing 1-vinylimidazole (28.23 g, 300 mmol), sodium tetrafluoroborate (33.0 g, 300 mmol) was added dropwise 27 ml (360 mmol) of bromoethane at 0 °C. The mixture was put into oil bath and stirred for 12 h at 40 °C. Then 150 ml of acetonitrile was added, and the mixture refluxed for 3 h. After cooling to room temperature, the precipitate was filtered and the filtrate was concentrated under reduced pressure. The residue was dissolved in dichloromethane and washed three times with deionized water. The solution was dried over sodium sulfate, filtered and concentrated. Drying the residue under high vacuum at 50 °C for 3 h gave the pure product. Yield 51.0 g (87 %).
^{1}H NMR (600 MHz, dmso-d6): 1.41 (t J=7.34 Hz, 3H), 3.83 (s, 3H), 4.18 (q, J=7.31 Hz, 2H) 5.41 (dd, J=8.80, 2.38 Hz, 1H), 5.94 (dd, J=15.68, 2.38 Hz, 1H), 7.26 (dd, J=15,63, 8,76 Hz, 1H), 7.91 (t, J=1,65 Hz, 1H), 8.17 (t, J=1.70 Hz, 1H), 9.45 (s, 1 H)
^{13}C NMR (151 MHz, dmso-d6): 15.49, 36.12, 44.58, 109.04, 119.56, 123.69, 129.31, 135.73.

2.4. Synthesis of poly(1-ethyl-3-vinylimidazolium tetrafluoroborate), (PIL-BF_4)

To a 250 ml flask containing stir bar, 1-ethyl-3-vinylimidazolium tetrafluoroborate (43.4,

210 mmol) and 100 ml of ethanol 0.68 g (4 mmol) of 2,2′-azobis(2-ethylpropionitrile) (AIBN) was added. The flask was put into pre-heated to 80 °C oil bath and connected to the argon line. The mixture was stirred at the same temperature for 16 h. After cooling the mixture was decanted, the residue was dissolved by acetonitrile (50 ml). The solution was poured into a beaker with 400 ml of tetrahydrofuran. The precipitated product was filtered, washed with THF and dried under a high vacuum for 12 h at 80 °C. Yield 36.7 g (85%).
^{1}H NMR (600 MHz, dmso-d6): 1.31-1.41 (m, 3H), 2.01-2.65 (m, 2H), 3.76-3.82 (m, 2H), 4.08-4.16 (m, 1H), 6.96 – 7.90 (m, 2H), 9.07-9.43 (m, 1 H)

2.5. Membrane characterization

The PVDF membranes were soaked in 1-ethyl-3-methylimidazolium tetrafluoroborate ($EMImBF_4$) at 100 °C for 1 h. The excess of electrolyte on the surface was collected by filter paper absorption. The procedure was repeated three times to achieve constant uptake value. The electrolyte uptake is calculated by

$$W\ (wt.\%) = (m_s/m_0 - 1)\times 100\%,$$

where m_0 is the weight of dry membrane, m_s is the weight of the saturated membrane. The ionic conductivity of PGEs was calculated from electrochemical impedance spectroscopy data over the frequency range from 0.1 Hz to 5 MHz using a P-45X potentiostat/galvanostat equipped with FRA-24M module (Electrochemical Instruments). The samples were sandwiched between symmetrical cells containing two steel electrodes with an area of A (0.785 cm^2 for Novacontrol and 0.281 cm^2 for FRA-24M) at the constant potential of 5 mV to measure membrane impedance, Z (Ω). The thickness of each sample was measured with a micrometer in five different points and the average value L (cm) was estimated for calculation. The conductivity (σ, S/cm) was determined by the equation:

$$\sigma = L/(Z\times A)$$

The membranes surfaces and cross-sections were analyzed by scanning electron microscope (SEM) in an TESCAN Vega 3 at 30 kV. Prior to analysis sample surfaces were gold-coated to achieve better image contrast. The membranes were fractured in liquid nitrogen for cross-section morphology observation. The differential scanning data were performed in TA Instruments Q20 V24.11 at a heating rate of 10 °C min^{-1} under N_2 atmosphere. The degree of crystallinity X_c was determined by

$$X_c\ (\%) = \Delta H_m/\Delta H_m^* \times 100\%,$$

where $\Delta H_m^* = 104.5$ J/g [29], is the enthalpy of fusion for total crystalline PVDF, ΔH_m is experimentally obtained value of the thermal effect from DSC data. The mechanical properties of the membranes were measured with the Universal Testing Machine (Instron 5985). A specimen was cut into small pieces (50×0.9 mm). All specimens were tested at room temperature. Two different approaches were used to determine the porosity of membranes. In the first case, the porosity (P_c) was calculated from the density of the membrane by the equation:

$$P_c = (1-\rho_m/\rho_p)\times 100\%,$$

where ρ_m is membrane density and ρ_p is the density of pure PVDF ($\rho_p = 1.77$ g/cm^3). The density of the membrane was calculated from its weight and its geometric dimensions. In the second case, to determine the porosity of the membrane was impregnated with n-butanol. Membrane samples were weighed (m_0) and placed in n-butanol for 12 h at 100 °C. Then the membranes were removed from the solvent and weighed in a saturated state (m_s). The porosity (P_b) was calculated by the following equation:

$$P_b = [(m_s-m_0)/\rho_b]/(m_0/\rho_p + (m_s-m_0)/\rho_b)\times 100\%,$$

where ρ_b and ρ_p are n-butanol (0.81 g/cm^3) and PVDF (1.77 g/cm^3) densities.

2.6. Preparation of Actuators

Bucky gel electrodes were prepared by the previously reported procedure [28]. The thickness of the obtained electrode film was 20–25 μm. Samples of the rectangular shape were cut from the membranes and electrodes. The polymer membranes were sandwiched between two bucky-gel electrodes via hot pressing. Each actuator was pressed separately. Three-layer films were activated by soaking in IL to constant mass. Finally, the actuators were cut to 20×10 mm for blocking force and 50×10 mm for tip displacement measurements.

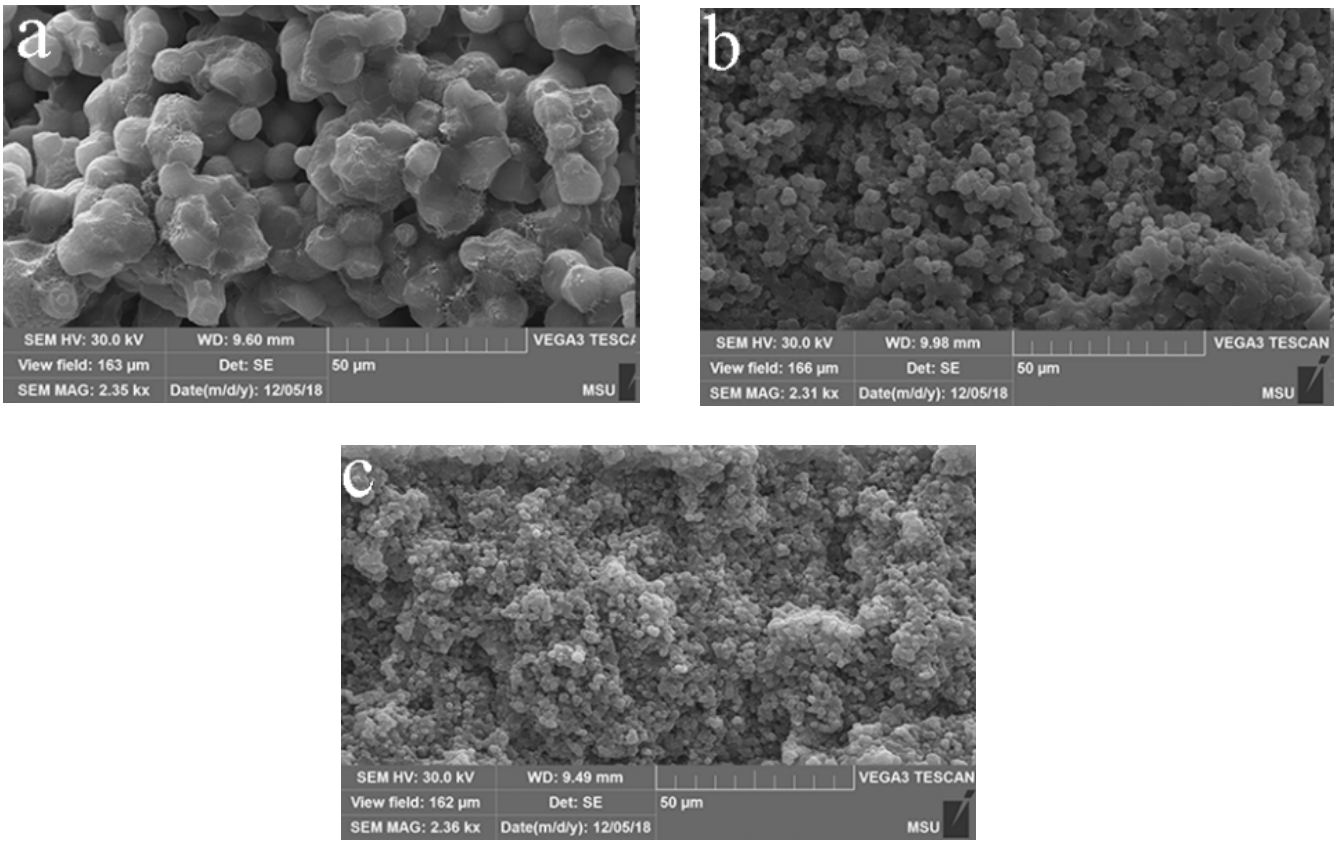

Fig. 1. SEM micrographs of cross-sections of PVDF membranes prepared with different DBP content: (a) 40 wt.%; (b) 50 wt.%; (c) 60 wt.%.

3. Results and discussion

3.1. Effect of formation conditions on membrane properties

PVDF is a semi-crystalline polymer, which is soluble only in some high boiling polar solvents such as *N,N*-dimethylacetamide, DMF, and *N*-methyl-2-pyrrolidone, and triethyl phosphate. All membranes in this work were prepared by dry-cast process from solutions in DMF, a good solvent for both PVDF and additives. Drying temperature and the rate of solvent evaporation both affect the degree of crystallinity of the polymer membrane [30]. It has recently been shown that the minimum degree of crystallinity can be achieved at a drying temperature of 80 °C using PIL-BF_4 as a pore-forming additive [28]. At the first stage of investigation, we prepared PVDF films at 80 °C with 40, 50 and 60 wt.% of dibutyl phthalate (DBP) content. Figure 1 shows the micrographs of the cross-section of the membranes after extraction of the additive. Unlike membranes prepared with PIL-BF_4 in this case the membranes had a spherulite structure. Not only chemical nature but also the concentration of additive affects phase separation and solidification of PVDF, namely rates of vitrification or crystallization processes. As can be seen in Fig. 1 the radius of spherulites decreases with increasing concentration of the additive.

Generally, additives such as non-solvents or pore-forming polymers are more soluble than PVDF. Upon solvent evaporation a homogeneous polymeric solution is separated into two phases. Initially, the phase, which consists of PVDF, forms a solid membrane structure, and the other phase occupies the remaining space. At the extraction step, additive removed from PVDF matrix leaving pores. In the case of the sample with 40 wt.% of DBP extraction of additive was incomplete. Analogous results were achieved for PIL-BF_4 [28]. Part of pore-forming additive was probably encapsulated in the PVDF matrix and remained in the membrane. On the other hand, a membrane with 60 wt.% DBP lost 63 wt.% during extraction, which indicates that part of the PVDF was encapsulated in the additive. Therefore, for further study membranes with 50 wt.% of additives were prepared and tested.

3.2. Effect of different additives on membrane properties

A series of PVDF membranes was prepared to compare the effect of commonly used additives with PIL-BF_4 on membrane properties. Polyethylene glycols with average masses 3000 and 40000 (PEG-3K and PEG-40K respectively), DBP and PIL-BF_4 were used as pore-forming additives. All membranes were cast at the same conditions (50 wt.% of additives at 80 °C). After extraction of additives, the membranes were analyzed by DSC and FTIR methods. The data are represented in Table 1.

Although the membranes are characterized by similar melting points, they differ significantly in both the degree of crystallinity and the composition of the crystalline phases. The membrane obtained with PIL-BF_4 shows the lowest degree of crystallinity. The crystalline phase composition of PVDF could be determined by FTIR spectra [31]. Analysis of the FTIR spectra of the membranes showed the presence of γ-polymorph in all cases. Characteristic bands of α-phase at 766, 795, 855 cm^{-1} are not presented on all FTIR spectra of the membranes. The β and γ-phases show a similar number of bands [32], both polymorphs characterized by the band at 840 cm^{-1}, however, it is stronger for the β-phase and for the γ-phase it appears as a shoulder of the band at 833 cm^{-1}. More distinguishable absorption bands of β- and γ-phases are at 1279 and 1234 cm^{-1} respectably.

The structure of the membranes was investigated by SEM analysis. The morphology of the membranes varies significantly depending on the selected pore-forming additive (see Fig. 2). Cross section SEM micrographs reveal evenly distribution of porosity throughout the membranes. The membranes prepared with PEGs and DBP have interconnected spherulite structure and the radius of the spherical fragments depends on the additive. On the contrary, the membrane obtained with PIL-BF_4 has a sponge-like structure. This difference in the structure probably explains the significant difference in the degree of crystallinity of the membranes. In the casting mold, one surface is always in contact with air, and the other is in contact with the substrate, which may lead to the difference in morphology of the surfaces. During evaporation of the solvent on the surface of the substrate, the concentration of the polymer can occur, leading to a surface gelling into a dense skin upon coagulation. The SEM images do not reveal a significant difference between surfaces in cases of PEGs and DBP, while in the case of PIL-BF_4, the lower surface looks denser.

Even though the pore-forming additives have different densities and were added in equal masses, the porosity values of all the membranes are almost the same (see Table 2). All membranes were activated by soaking in IL to measure ionic conductivity. It should be noted that the membrane obtained using PEG-40K showed the maximum electrolyte uptake. Besides, the membrane was too fragile. It was disintegrated when placed between the electrodes, so the ionic conductivity was not measured. The results of the measurement of the rest of the membranes are presented in Table 2.

Table 1
DSC data, degree of crystallinity and crystalline phase composition of PVDF

Additive	T_m, °C	ΔH_m, J/g	Crystallinity[a]	Crystalline phases[b]
PEG-3K	165	61.97	59%	γ phase
PEG-40K	167	60.64	58%	γ phase
DBP	161	67.95	65%	β+ γ phases, mostly γ
PIL-BF4	165	40.37	39%	β+ γ phases, mostly β

[a]Crystallinity calculated from enthalpy from DSC data; [b] Crystalline phase were determined by FTIR.

Table 2
Porosities, electrolyte uptakes and ionic conductivities of PVDF membrane

Additive	$P_{c,\%}$	$P_{b,\%}$	Electrolyte uptake, wt.%	Uptake by volume, %	σ, $mScm^{-1}$	T
PEG-3K	45	45	89	55	1.16	2.6
PEG-40K	46	47	96	56	-	-
DBP	46	46	75	51	1.43	2.1
PIL-BF4	48	51	117	62	1.36	2.2

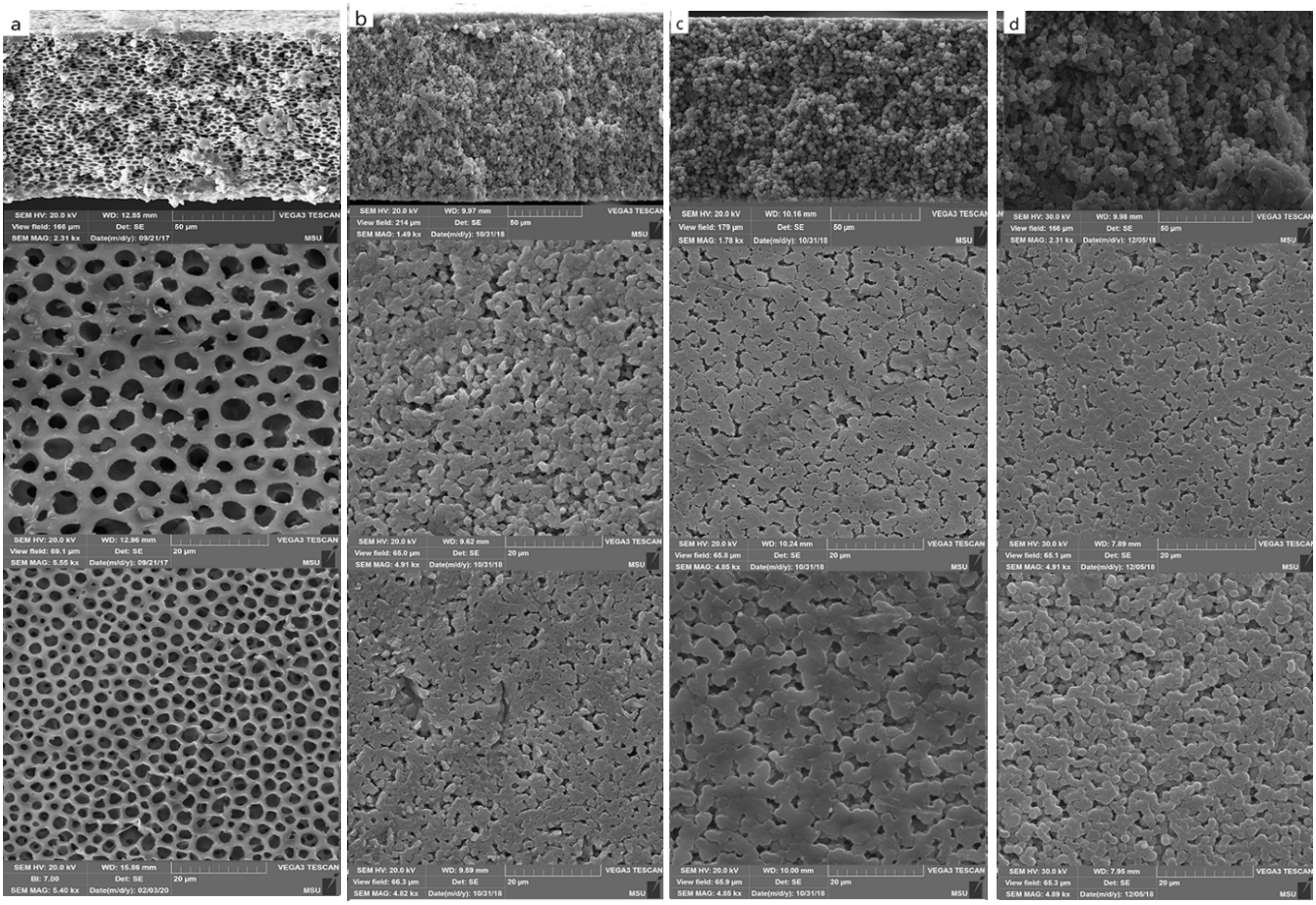

Fig. 2. SEM micrographs of cross-sections (top), lower (middle) and upper surfaces (bottom) of PVDF membranes prepared with different additives: (a) PIL-BF_4; (b) PEG-3K; (c) PEG-40K and (d) DBP.

All membranes were soaked in $EMImBF_4$ to define electrolyte uptake and ionic conductivities. After electrolyte impregnation, the size of all membranes remained practically unchanged. However, electrolyte uptakes calculated by volume exceed the porosity values in all cases (Table 2). This difference arises because the amorphous PVDF phase is capable of absorbing electrolyte. The maximum difference in volume uptake and porosity was observed for a membrane with a minimum degree of crystallinity, and vice versa, a membrane with a minimum degree of crystallinity had closer volume uptake and porosity. There is no increase in ionic conductivity with an increase in electrolyte absorption, which may also indicate that part of the IL is trapped by the amorphous PVDF phase. Despite those effective porosities of all membranes are close, it is pore interconnectivity and membrane morphology that defines the final ion conductivity. To assess the shortest distance from one surface to another through a porous structure, tortuosity (T) can be calculated [22, 33]. For PGE not containing ionomers, tortuosity is calculated by the equation [17]:

$$T = \sqrt{\sigma_0 / \sigma \times \mathrm{P}},$$

where σ_0 and σ are the conductivities of neat $EMImBF_4$ (13.6 $mScm^{-1}$) and the membrane, respectively, P is effective membrane porosity.

The mechanical properties of the membranes were determined by stretching. Stress-strain curves of dry and saturated in $EMImBF_4$ membranes are shown in Fig. 3. Dry PVDF membrane prepared with PIL-BF_4 was the strongest membrane yielding the greatest modulus. Generally, the membrane demonstrates high mechanical properties. Tensile strength of the membrane two-fold higher than for other membranes. Tensile modulus is comparable even with anisotropic electrospun aligned PVDF fibrous membranes [34].

The values of the mechanical properties of dry and saturated in IL membranes are provided in Table 3. The elastic modulus of wet membranes dropped significantly with respect to the dry membranes. In the case of membranes prepared from PEG and DBP, the decrease in the modulus is much greater. The degree of crystallinity in these mem-

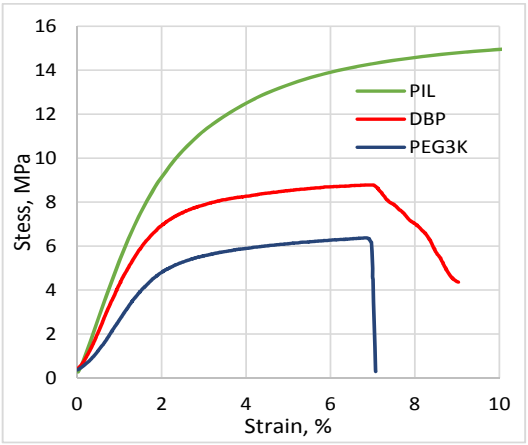

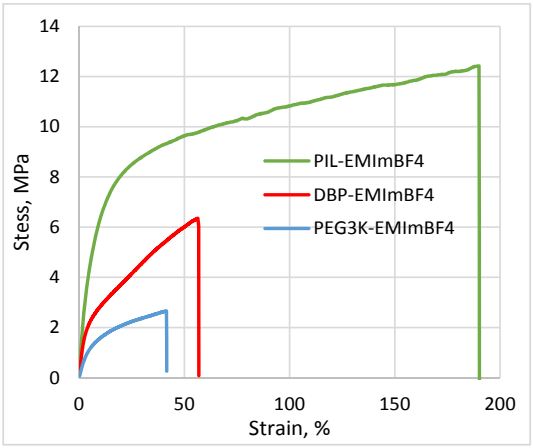

Fig. 3. Strain-stress curves of dry and saturated PVDF membranes.

branes is higher, and the degree of impregnation in all membranes is about the same. The reason for this effect is probably related to the morphology of the membranes. The spherulites are connected mostly by the amorphous phase, which can absorb the electrolyte, which leads to a decrease in the modulus of the membrane.

3.3. Bucky-gel actuators fabrication and performance

Bucky gel actuators were made based on all membranes for the electromechanical tests. The actuators were fabricated via hot-pressing according to slightly modified literature procedure [35]. According to the theory of bending of a three-layer bucky-gel actuator [26, 35], the rigidity of the electrolyte layer has a slight effect on the deformation of the actuator, and generated force depends only on the Young's modulus of electrodes. The mechanical properties of used electrodes are presented in Table 3. The thickness of the actuator, and especially the thickness of the electrodes, significantly affect both maximum tip displacement and the blocking force. Therefore, actuators of the same size (20×10×0.30 mm) were fabricated for testing. The blocking force was measured using analytical balances similar to the method described elsewhere [36]. Time dependence of blocking forces for the actuators are shown in the Fig. 4. All measurements were carried out at a constant voltage of 3 V.

It can be seen in the Fig. 4, the rate of occurrence of the blocking force correlates with the ionic conductivity of the membranes. Although all the actuators were made with the same electrodes, the maximum blocking force for them varies considerably. This is probably since in the process of pressing a dense layer is formed at the interface between the membrane and the electrode. When voltage is applied, an electrical double layer forms near the electrode interface in the membrane, and not inside the porous electrode. Therefore, in our case, a membrane with a larger elastic modulus generates a larger force. Further studies were carried out with a membrane prepared using PIL-BF_4. To measure the maximum tip displacement, an actuator with geometrical dimensions 50×10 mm was fabricated. The maximum deformation of 1.35% is achieved in 120 sec at a voltage of 3 V (see Fig 4). It is worth noting that after reaching the maximum displacement, the effect of back relaxation was practically not observed. Actuators with different ILs were manufactured and tested at different voltages.

Table 3

Mechanical properties of PVDF membranes prepared with different pore-forming additives

Electrolyte	PEG-3K	DBP	PIL-BF_4	Electrode
Electrolyte Modulus, MPa	263.2 (31.7)[a]	426.3 (74.4)	538.3 (138.3)	756.9 (489.5)
Tensile strength, MPa	6.4 (4.1)	8.8 (6.3)	17.7 (12.4)	27.4 (17.7)
Fracture strain, %	7.0 (41.5)	9.0 (56.8)	132.5 (190.0)	14.0 (13.6)
Thickness, μm	105 (130)	104 (116)	105 (130)	25 (25)

[a]The values of the mechanical properties of saturated membranes and electrode are shown in brackets.

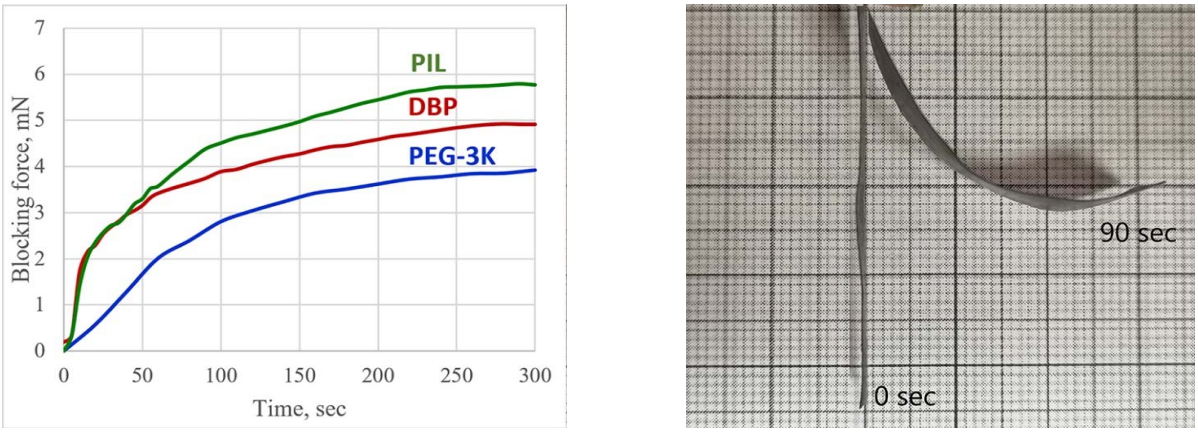

Fig. 4. Diagram of time dependence of blocking forces (on the left) and image of bending of the actuator based on membrane prepared with PIL-BF_4 (on the right).

The results are summarized in Table 4. Time required to achieve the maximum blocking force is shown in brackets. The actuators demonstrates electromechanical properties comparable to modern works on bucky-gel actuators [37, 38].

Table 4
Maximum blocking force values of the actuators

U, V	$EMImBF_4$	$BMImBF_4$	EMImTFSI
2 V	4.2 mN (460 s)	5.1 mN (690 s)	3.1 mN (580 s)
3 V	5.8 mN (240 s)	7.1 mN (540 s)	4.2 mN (480 s)
4 V	6.8 mN (180 s)	8.5 mN (390 s)	4.9 mN (610 s)

4. Conclusions

Microporous PVDF membranes were prepared via dry-cast technique from DMF solution using different pore-forming additives, namely PIL-BF_4, DBP, PEG-3K and PEG-40K. According to SEM analysis all membranes have pores open to both surfaces and porosity is evenly distributed throughout the membranes. The chemical nature of the additive has been shown to have a significant effect on the morphology, physical, mechanical and electrochemical properties of the membranes. The membranes prepared with PEGs and DBP have interconnected spherulite structure which lead to high degree of crystallinity. Oppositely, the membrane prepared with PIL-BF_4 has a sponge-like structure with low PVDF crystallinity and as a result this membrane demonstrates the highest electrolyte uptake of 117 wt.%. The membrane prepared with PIL-BF_4 also demonstrates a high mechanical properties, namely tensile modulus is 538 MPa and fracture strain is 133%. The actuators with bucky-gel electrodes based on the membranes prepared with different additives were fabricated. The maximum blocking force values generated at 3 V DC by actuators prepared with PIL-BF_4, DBP and PEG-3K were 5.8, 4.9 and 3.9 mN respectively. The actuator fabricated with PIL-BF_4 exhibited a competitive blocking force compared with recently reported actuators. Thus, we have shown that the structure and mechanical properties of membranes have no less impact on the performance of actuators than electrodes.

Acknowledgment

The reported study was funded by RFBR according to the research project № 18-29-18090. Authors are grateful to the Moscow State University (Russia) for the opportunity to use the NMR facilities of the Center for Magnetic Tomography and Spectroscopy.

References

[1]. Z.-W. Ouyang, E.-C. Chen, T.-M. Wu, *Materials* 8 (2015) 4553–4564. DOI: 10.3390/ma8074553
[2]. B. Jaleh, N. Gavar, P. Fakhri, N. Muensit, S.M. Taheri, *Membranes* 5 (2015) 1–10. DOI: 10.3390/membranes5010001
[3]. C.S. Ong, W.J. Lau, B. Al-anzi, A.F. Ismail, *Membrane Water Treatment* 8 (2017) 211–223. DOI: 10.12989/mwt.2017.8.3.211
[4]. R. Faiz, M. Fallanza, S. Boributh, R. Jiraratananon, I. Ortiz, K. Li, *Chem. Eng. Sci.* 94 (2013) 108–119. DOI: 10.1016/j.ces.2013.02.048

[5]. V.K. Tiwari, P.K. Kulriya, D.K. Avasthi, P. Maiti, *ACS Appl. Mater. Interfaces* 1 (2009) 311–318. DOI: 10.1021/am800040q
[6]. Guo-dong Kang, Yi-ming Cao, *J. Memb. Sci.* 463 (2014) 145–165. DOI: 10.1016/j.memsci.2014.03.055
[7]. Z. Xie, M. Hoang, T. Duong, D. Ng, P. Singh, P. Ray, A.V.R. Reddy, K. Parashuram, S. Maurya, *J. Mater. Sci. Res.* 1 (2012) 37–44. DOI: 10.5539/jmsr.v1n1p37
[8]. A.C.M. Franken, J.A.M. Nolten, M.H.V. Mulder, D. Bargeman, C.A. Smolders, *J. Memb. Sci.* 33 (1987) 315–328. DOI: 10.1016/S0376-7388(00)80288-4
[9]. Y. Zhang, J. Sunarso, S. Liu, R. Wang, *Int. J. Greenh. Gas Control.* 12 (2013) 84–107. DOI: 10.1016/j.ijggc.2012.10.009
[10]. R. Khalilpour, K. Mumford, H. Zhai, A. Abbas, G. Stevens, E.S. Rubin, *J. Clean. Prod.* 103 (2015) 286–300. DOI: 10.1016/j.jclepro.2014.10.050
[11]. Y. Gao, *Nanoscale Res. Lett.* 12 (2017) 387. DOI: 10.1186/s11671-017-2150-5
[12]. Y. Xin, H. Sun, H. Tian, C. Guo, X. Li, S. Wang, C. Wang, *Ferroelectrics* 502 (2016) 28–42. DOI: 10.1080/00150193.2016.1232582
[13]. R. Mejri, J.C. Dias, S.B. Hentati, M.S. Martins, C.M. Costa, S. Lanceros-Mendez, *J. Non. Cryst. Solids* 453 (2016) 8–15. DOI: 10.1016/j.jnoncrysol.2016.09.014
[14]. R.Hagiwara, J.S. Lee, *Electrochemistry* 75 (2007) 23–34. DOI: 10.5796/electrochemistry.75.23
[15]. S.S. Zhang, *J. Power Sources* 164 (2007) 351–364. DOI: 10.1016/j.jpowsour.2006.10.065
[16]. Q. Cheng, Z. Cui, J. Li, S. Qin, F. Yan, J. Li, *J. Power Sources* 266 (2014) 401–413. DOI: 10.1016/j.jpowsour.2014.05.056
[17]. P. Arora, Z. Zhang, *Chem. Rev.* 104 (2004) 4419–4462. DOI: 10.1021/cr020738u
[18]. J.T. Jung, J.F. Kim, H.H. Wang, E. di Nicolo, E. Drioli, Y.M. Lee, *J. Memb. Sci.* 514 (2016) 250–263. DOI: 10.1016/j.memsci.2016.04.069
[19]. C.H. Du, Y.Y. Xu, B.K. Zhu, *J. Appl. Polym. Sci.* 114 (2009) 3645–3651. DOI: 10.1002/app.30105
[20]. Z.-C. Zhang, C.-G. Guo, J-.L. Lv, *Polymers & Polymer Composites* 23 (2015) 175–180.
[21]. J.-H. Kim, K.-H. Lee, *J. Memb. Sci.* 138 (1998) 153–163. DOI: 10.1016/S0376-7388(97)00224-X
[22]. J.H. Cao, B.K. Zhu, Y.Y. Xu, *J. Memb. Sci.* 281 (2006) 446–453. DOI: 10.1016/j.memsci.2006.04.013
[23]. H. Bin Li, W.Y. Shi, Y.F. Zhang, D.Q. Liu, X.F. Liu, *Polymers* 6 (2014) 1846–1861. DOI: 10.3390/polym6061846
[24]. L. Guo, Y. Liu, C. Zhang, J. Chen, *J. Memb. Sci.* 372 (2011) 314–321. DOI: 10.1016/j.memsci.2011.02.014
[25]. R. Sahrash, A. Siddiqa, H. Razzaq, T. Iqbal, S. Qaisar, *Heliyon* 4 (2018) E00847. DOI: 10.1016/j.heliyon.2018.e00847
[26]. T. Fukushima, K. Asaka, A. Kosaka, T. Aida, *Angew. Chem. Int. Edit.* 44 (2005) 2410–2413. DOI: 110.1002/anie.200462318
[27]. O. Kim, S.Y. Kim, B. Park, W. Hwang, M.J. Park, *Macromolecules* 47 (2014) 4357–4368. DOI: 10.1021/ma500869h
[28]. O.S. Morozov, S.S. Shachneva, A.V. Kepman, *IOP Conf. Ser. Mater. Sci. Eng.* 683 (2019) 012060. DOI: 10.1088/1757-899X/683/1/012060
[29]. W. Ma, J. Zhang, X. Wang, S. Wang, *Appl. Surf. Sci.* 253 (2007) 8377–8388. DOI: 10.1016/j.apsusc.2007.04.001
[30]. D.L. Chinaglia, R. Gregorio, J.C. Stefanello, R.A.P. Altafim, W. Wirges, F. Wang, R. Gerhard, *J. Appl. Polym. Sci.* 116 (2010) 785–791. DOI: 10.1002/app.31488
[31]. P. Martins, A.C. Lopes, S. Lanceros-Mendez, *Prog. Polym. Sci.* 39 (2014) 683–706. DOI: 10.1016/j.progpolymsci.2013.07.006
[32]. T. Boccaccio, A. Bottino, G. Capannelli, P. Piaggio, *J. Memb. Sci.* 210 (2002) 315–329. DOI: 10.1016/S0376-7388(02)00407-6
[33]. E. Quartarone, P. Mustarelli, A. Magistris, *J. Phys. Chem. B.* 106 (2002) 10828–10833. DOI: 10.1021/jp0139843
[34]. H. Na, Q. Li, H. Sun, C. Zhao, X. Yuan, *Polym. Eng. Sci.* 49 (2009) 1291–1298. DOI: 10.1002/pen.21368
[35]. K. Mukai, K. Asaka, K. Kiyohara, T. Sugino, I. Takeuchi, T. Fukushima, T. Aida, *Electrochim. Acta* 53 (2008) 5555–5562. DOI: 10.1016/j.electacta.2008.02.113
[36]. H. Tamagawa, K. Yagasaki, F. Nogata, *J. Appl. Phys.* 92 (2002) 7614–7618. DOI: 10.1063/1.1516269
[37]. K. Asaka, K. Mukai, I. Takeuchi, K. Kiyohara, T. Sugino, N. Terasawa, K. Hata, T. Fukushima, T. Aida, *Proc. SPIE 7037, Carbon Nanotubes and Associated Devices* (2008) 703710. DOI: 10.1117/12.794503
[38]. A. Simaite, B. Tondu, F. Mathieu, P. Souéres, C. Bergaud, *Proc. SPIE 9430, Electroactive Polymer Actuators and Devices* (EAPAD) (2015) 94301E. DOI: 10.1117/12.2083936